Pergamon

J. Aerosol Sci., Vol. 25, No. 1, pp. 75–90, 1994

0021-8502/94 $6.00+0.00

THE MEASUREMENT OF THE FRACTAL DIMENSION OF INDIVIDUAL *IN SITU* SOOT AGGLOMERATES USING A MODIFIED MILLIKAN CELL TECHNIQUE

S. NYEKI and I. COLBECK

Inst. Environmental Research, Chemistry Department, University of Essex, Colchester, Essex CO4 3SQ, U.K.

(*Received* 16 *April* 1993; *and in final form* 22 *July* 1993)

Abstract—A method is presented, using a modified Millikan cell, to measure the fractal dimension (D) of *in situ* carbonaceous agglomerates in three dimensional space. From the measured aerodynamic diameter (sedimentation technique) and the mass of the agglomerate (photoelectric technique), D of an individual agglomerate is derived. Results, in the range of $1.87 \leqslant D \leqslant 2.19$, were in good agreement with those of several theories and calibration against polyvinyltoluene spheres which gave $2.96 \leqslant D \leqslant 2.99$.

Agglomerate re-structuring by the electric field was observed and deliberately induced in two agglomerates to give $D = 2.11$ and 2.19. This mechanism was deduced to be responsible for the high values observed in D.

NOMENCLATURE

B	buoyant force due to the displacement of the medium gas by the particle
$C(d_{AE})$	slip correction factor for a particle diameter d_{AE}
$C(d_{ME})$	slip correction factor for a particle diameter d_{ME}
$C(d_{VE})$	slip correction factor for a particle diameter d_{VE}
d_{ADJ}	adjusted sphere diameter
d_{AE}	aerodynamic diameter
$d_{AE,\parallel}$	aerodynamic diameter of a particle aligned vertically
d_{GE}	diameter of a sphere enclosing the particle
d_H	hydrodynamic diameter
d_{ME}	mobility equivalent diameter
d_0	primary spherule diameter
d_{VE}	volume equivalent diameter
D	mass fractal dimension calculated from $2r_G$
D_H	mass fractal dimension calculated from d_H
e	fundamental electronic charge, $1.6021892 \times 10^{-19}$ Coulomb
$E_{B,i}$	balance electric field for a particle with n_i charges
$E_{B,i+1}$	balance electric field for a particle with n_{i+1} charges
E_i	electric field imparting an upward velocity v_i to a particle
F	friction coefficient on a particle
F_D	drag force on a particle
g	acceleration due to gravity, 9.813 ms^{-2} at 53°N
Kn	Knudsen number
l	Millikan plate separation
m	mass of a primary spherule
M	total mass of the particle
n	number of elementary charges on the particle
N	number of primary particles in the agglomerate
r_i	distance of m_i from the centre of gravity
r_G	radius of gyration
v_i	upward velocity of a particle in an electric field E_1
v_{IRR}	settling velocity of an irregularly shaped particle
v_{TS}	the terminal settling velocity with the particle aligned in its preferred orientation for sedimentation under gravity alone
$v_{TS,\parallel}$	the terminal settling velocity with the particle long axis aligned vertically and calculated for sedimentation under gravity alone
v_{VE}	settling velocity of a volume equivalent sphere
$V_{B,i}$	balance electric field for a particle with n_i charges
$V_{B,i+1}$	balance electric field for a particle with n_{i+1} charges
η	gas viscosity, 1.83245×10^{-9} kg m^{-1} s^{-1} at 23°C
λ	gas mean free path, 0.0673 μm at 1013 mbar and 23°C
ρ_{MEDIUM}	density of the gas medium
ρ_0	density of a primary spherule
ρ_p	density of the particle

ρ_w unit density
τ particle relaxation time
χ dynamic shape factor with no electric field and for Kn > 0
$\chi_{||}$ dynamic shape factor for a particle aligned vertically in an electric field and for Kn > 0

INTRODUCTION

Clusters may be described by various fractal dimensions; these include relationships between the number of primary particles and the radius of gyration, the density of primary particles about the centroid of the agglomerate, the perimeter fractal (Kaye, 1984) and the pair correlation function (Forrest and Witten, 1979). Virtually all experimental determinations of the fractal dimension (D) of agglomerates are based on calculations of electron or optical microscope images (Kaye *et al.*, 1987; Samson *et al.*, 1987; Gentry *et al.*, 1988). However there is still a question as to whether D determined from projections is related to its three-dimensional value.

Methods suitable to measure D in three dimensions include tempering (Schmidt-Ott, 1988a) and optical structure measurements (Schaefer *et al.*, 1984; Martin *et al.*, 1986; Hurd and Flower, 1988). The tempering method involves measuring aerodynamic radii before and after heat treatment; however the technique is only valid for $D > 2$ in the free molecular regime. The thermally induced restructuring of agglomerates was further investigated by the use of a low-pressure impactor and a differential mobility analyzer to determine D for silver agglomerates in the size range 10–100 nm (Kütz and Schmidt-Ott, 1990).

More recently D has been determined *in situ* using a variety of techniques simultaneously (Weber, 1992). The central feature was the use of inductively-coupled plasma optical emission spectrometry (ICP-OES), to measure the agglomerate mass.

Optical structure measurements have also proved successful. Zhang *et al.* (1988) found values of $D = 1.62$ and $D = 1.72$ for light-scattering and transmission electron microscope measurements, respectively.

Despite these successful techniques, great effort and time are still required to measure the fractal dimension of an ensemble of agglomerates. To our knowledge measurements of D for single agglomerates in three dimensions have not appeared in the literature. In this paper a modified Millikan cell or MMC (Allen and Raabe, 1985a; Colbeck *et al.*, 1989a) is described in which the *in situ* measurement of D for single agglomerates in the transition/continuum regime is determined.

The method relies on the measurement of the aerodynamic diameter and the absolute mass of the agglomerate using a photoemission method (Arnold, 1979; Philip *et al.*, 1983). Hence the volume equivalent diameter (d_{VE}) and the measured aerodynamic diameter (d_{AE}) allow the dynamic shape factor (χ) and the mobility equivalent diameter (d_{ME}) to be calculated. The latter diameter is equivalent to the hydrodynamic diameter (d_H). The relationship between d_H and the radius of gyration r_G has been investigated both theoretically and experimentally and may then be used to derive the fractal dimension.

The only parameters required for these determinations are an accurate estimation of the sedimentation velocity and various balance voltages in the MMC.

THEORY

A discussion of the theory for the MMC is first treated by defining the relevant equations, namely the particle sedimentation velocity, volume equivalent diameter, dynamic shape factor (with and without a preferential orientation), the mobility equivalent diameter and the fractal dimension.

Several authors (Berry, 1989; Magill, 1991; Naumann and Bunz, 1991) have considered the aerodynamic properties of agglomerates. These theories are discussed and evaluated allowing their subsequent inter-comparison using the results obtained from this investigation.

THE MODIFIED MILLIKAN CELL

The particle balance equation

Consider a particle balanced in a d.c. electric field. The gravitational force therefore equals the force due to the electric field, and

$$Mg - B = n_i e E_{B,i}, \tag{1}$$

where the buoyancy force B, although negligible ($\rho_{MEDIUM}/\rho_p < 10^{-3}$ for most solids and liquids), has been included for consistency. It is a straightforward task to balance the particle and measure $E_{B,i}$ which is defined as $V_{B,i} l^{-1}$, where V represents the voltage between the d.c. plates and l is the plate separation.

Under gravity alone the sedimentation velocity of the particle is given by equation (2) (Hinds, 1982) and may be measured by an accurate determination of the time

$$v_{TS} = \frac{(\rho_p - \rho_{med}) g d_{VE}^2 C(d_{VE})}{18\eta\chi} = \frac{\rho_w g d_{AE}^2 C(d_{AE})}{18\eta}, \tag{2}$$

where χ is the dynamic shape factor which is discussed further below. If an electric field is applied to a balanced particle such that the particle acquires an upward velocity v_i then equation (1) becomes

$$Mg + 3\pi\eta v_i d_{AE} = neE_i, \tag{3}$$

where the second term is the Stokes drag on a particle. If several values of the upward velocity in different electric fields are measured then a regression plot gives an accurate determination of $E_{B,i}$ and the terminal settling velocity with the particle long-axis aligned vertically, $v_{TS,\parallel}$. From the regression plot $v_{TS,\parallel}$ may be calculated for sedimentation under gravity alone when $v_i = 0$.

If the particle is then subjected to u.v. light and one or more electrons are emitted the particle may again be balanced, but at a different electric field. Thus

$$Mg = n_{i+1} e E_{B,i+1}. \tag{4}$$

By measuring the balance voltage before and after emission several times, the absolute mass (M) and charge state of the particle may be determined. If a single electron from a negative particle is removed, then

$$n_{i+1} = n_i - 1. \tag{5}$$

Hence, solving for the mass and the charge state, it may be determined that

$$M = \frac{e V_{B,i} V_{B,i+1}}{|gl(V_{B,i+1} - V_{B,i})|}, \tag{6}$$

$$n_i = \frac{e V_{B,i+1}}{|V_{B,i+1} - V_{B,i}|}. \tag{7}$$

From equation (7) the charge state may be determined even if the balance voltages are not properly calibrated or the plate separation is known.

The dynamic shape factor

For particle shapes other than spherical a correction factor is applied to Stokes' law to account for the effect of shape on particle motion. The dynamic shape factor for a randomly orientated sedimenting particle in the transition regime is given by (Kasper, 1982)

$$\chi = \frac{\rho_p d_{VE}^2 C_{VE}}{\rho_0 d_{AE}^2 C_{AE}}. \tag{8}$$

The agglomerates investigated in this study were observed to be generally isometric for which χ is similar in all orientations. If d^2_{AE} is substituted for $d^2_{AE,\|}$ then $\chi_\|$ (the dynamic shape factor for the particle long-axis aligned with the electric field) is given. An additional form of equation (8) is

$$\chi = \frac{d_{ME} C_{VE}}{d_{VE} C_{ME}}, \tag{9}$$

where d_{ME} is the mobility equivalent diameter and the slip correction factors are given by the Knudsen–Weber formula

$$C = 1 + \mathrm{Kn}(\alpha + \beta \exp(-\gamma/\mathrm{Kn})), \tag{10}$$

where Kn is the Knudsen number defined as the gas mean free-path (λ) divided by the particle radius. For the transition regime Kn varies in the range $0 < \mathrm{Kn} < 100$. Allen and Raabe (1985a) investigated polystyrene latex (PSL) and polyvinyltoluene (PVT) particles and found that (for $\lambda = 0.0673$ μm, 1013 mbar and 23°C) $\alpha = 1.142$, $\beta = 0.558$ and $\gamma = -0.999$.

Equation (10) may be simplified by eliminating the exponential term, and the resulting error is only 0.1% in C for a 0.5 μm particle. As particles with d_{AE} in excess of 0.8 μm have been investigated the estimation is reasonable.

When considering agglomerates the difficulty arises as to which diameter to use in the Knudsen–Weber formula. The drag force on an agglomerate may be expressed (Allen and Raabe, 1985b) as

$$F_D = \frac{3\pi\eta d_{VE} v \chi}{C(d_{VE})}. \tag{11}$$

However reported values of χ have shown it to be a function of the Knudsen number (Allen and Raabe, 1985b) and hence the diameter. Experiments on doublets and triplets by Cheng *et al.* (1988) supported the use of an adjusted sphere diameter (Dahneke, 1973) which gave the same drag force on the particle

$$F_D = \frac{3\pi\eta d_{VE} v \chi_0}{C(d_{ADJ})}, \tag{12}$$

where χ_0 is the dynamic shape factor in the continuum regime.

However such considerations may be avoided here if equation (8) is considered further in the form

$$\chi = V_{VE}/V_{IRR}. \tag{13}$$

The velocity of the irregular shaped particle is given experimentally while V_{VE} (by definition for a sphere) is derived from the mass of the particle. Thus the dynamic shape factor (for $\mathrm{Kn} > 0$) may be determined independently of the reliance on slip correction (Kasper, 1982).

The determination of the fractal dimension

The calculation of D is a straightforward task when a log–log plot of N vs $2r_G/d_0$ is performed. As a consequence of such a method, D is calculated for an ensemble of agglomerates and it is generally assumed that all agglomerates possess the same value of D. In the reported method here, D is found for individual agglomerates and therefore an exact equation, equation (14), relating N to a characteristic length is required. Large agglomerates may be described as mass fractals and obey a power law relation between mass and r_G (Mountain and Mulholland, 1988; Megaridis and Dobbins, 1990); thus

$$N = \varepsilon(2r_G/d_0)^D, \tag{14}$$

where N is the number of primary spherules in the agglomerate and ε is a dimensionless prefactor, commonly assigned a value of unity in the literature. However this may not

always be the case and will be discussed further. In addition the relationship between r_G and d_H requires investigation if d_H is to be used as a characteristic length.

Determination of the pre-factor ε. Simulations by Mountain and Mulholland (1984) gave values of ε as 0.82 for $D=1$, 1.15 for $D=2$ and 1.11 for $D=3$. A later simulation for the free molecular/transition regime (Mountain and Mulholland, 1988) found $\varepsilon=1.55$ when $D=1.90$, while Mulholland *et al.* (1988) gave $\varepsilon=1.30$ for $D=1.91$. Sorensen *et al.* (1992) derived an equation for ε as a function of D by considering the radius of gyration of a sphere as $N\to1$, giving $\varepsilon=(5/3)^{D/2}$, for agglomerates with $r_G\leqslant120$ nm. This model was found to give agreement with the Mountain and Mulholland (1988) simulation but differed slightly from that of Mulholland *et al.* (1988).

In summary the simulated value of ε ranges from approximately 1.15 to 1.67 for $1.8\leqslant D\leqslant2.0$, using $2r_G$ as the characteristic length and for the free molecular/transition regime.

Experimental values of ε have been determined for characteristic radii other than r_G. In experiments on soot particles, Megaridis and Dobbins (1990) used the Feret diameter and gave values of ε ranging from 0.92 to 1.14 for the free molecular/transition regime. An alternative interpretation of ε, by Schmidt-Ott (1988b), was as a filling factor for a close packed agglomerate. The expression

$$N=\varepsilon(d_{ME}/d_0)^D \tag{15}$$

was used with ε inferred to be 0.7 (Cargill, 1984) for the free molecular/transition regime. Furthermore, experiments by Sorenson *et al.* (1992) found that in the transition/continuum regime, $\varepsilon=1.56$ for agglomerates with $D=1.73$.

The relation between r_G *and* d_H. The mass weighted radius of gyration may be defined as

$$Mr_G^2=\sum_{i=1}(m_i r_i^2), \tag{16}$$

where r_i is the distance of a spherule of mass m_i from the agglomerate centre of gravity. Determinations of r_G are possible from electron microscope images and the optical static structure factor (Samson *et al.*, 1987). However r_G is not given by the MMC method and therefore must be derived by relation to an alternative characteristic size parameter. Tence *et al.* (1986) have shown that the radius of gyration, weighted (equation (16)) and unweighted by mass, and the Feret diameter (maximum particle diameter) give essentially similar values of D.

The characteristic diameter used in this paper is the hydrodynamic diameter defined by the friction coefficient (Meakin *et al.*, 1985)

$$F=3\pi\eta d_H. \tag{17}$$

The hydrodynamic diameter has also been found to fulfil equation (18) in the continuum regime (Mountain *et al.*, 1986; Wiltzius, 1987; Chen *et al.*, 1987)

$$N\sim d_H^{D_H}. \tag{18}$$

Simulations on different growth models have allowed D_H, the fractal dimension from equation (18), to be calculated, and these are compared to values of D in Table 1.

Investigations have shown that the theoretical and experimental relationship between d_H and $2r_G$ lies close to parity as a consequence of the flow field around the agglomerate. For $r_G\gg\lambda$ friction is caused by air flow around the agglomerate while for $r_G\ll\lambda$ friction is due to the impacts of air molecules on the primary spherules (Berry, 1989). Further investigations on the aerodynamic drag have been discussed by Mountain *et al.* (1986), Rogak and Flagan (1990) and Rogak *et al.* (1993).

In a paper by Meakin *et al.* (1985) simulations on diffusion-limited cluster–cluster (DLCC) aggregation gave a model of the form $d_H\sim(2r_G)^\delta$ where $\delta=0.895\pm0.395$ with $d_H=1.84\pm0.05$ and $2r_G=1.81\pm0.12$. A later simulation on reaction limited cluster–cluster

(RLCC) aggregation (Chen *et al.*, 1987) gave a ratio $d_H/2r_G \cong 0.97$, found to be almost independent of agglomerate size.

Simulations on the macroscopic hydrodynamic flow in the continuum regime by Mountain *et al.* (1986) gave an expression for the friction coefficient (F) which reduced to

$$F = 6\pi\eta r_G. \tag{19}$$

Comparison to equation (17) suggested that, due to the entrapment of the medium within the agglomerate, $2r_G$ and d_H were similar in the continuum regime. Hess *et al.* (1986) derived a relationship between $2r_G$ and d_H with the assumption that the agglomerate was spherically symmetric with a diameter d_{GE} (the diameter just enclosing the particle)

$$(d_H/2r_G)^2 = 4(2+D)(D-1)^2/D^3. \tag{20}$$

This simple model of a spherically symmetric fractal gave $1.21 \leqslant d_H/2r_G \leqslant 1.46$ for $1.7 \leqslant D \leqslant 2.1$ in the continuum regime and was shown to increase with D.

Experimental comparisons have been made for both DLCC and RLCC aggregation models. Measurement of the hydrodynamic diameter using light scattering gave $D_H = 1.75 \pm 0.03$ for DLCC aggregation (Bolle *et al.*, 1987; Cametti *et al.*, 1987), in good agreement with the simulated value of $D = 1.76 \pm 0.08$ (Meakin, 1984a). Rarity and Pusey (1986) investigated aggregating polystyrene spheres in the RLCC regime and reported $D_H = 2.02 \pm 0.05$ and $D = 2.1 \pm 0.05$.

However experiments by Wiltzius (1987) in the RLCC aggregation regime gave a ratio $d_H/2r_G = 0.72 \pm 0.02$ for 50–700 nm silica agglomerates. Fractal dimensions $D = 2.10 \pm 0.03$ and $D_H = 2.13 \pm 0.07$ were found, the former comparing favourably to simulated values in Table 1. An analysis by van Saarlos (1987) suggested that d_H was considerably lower than expected for spherically symmetric agglomerates and could be attributed to agglomerate asymmetry.

More recently in a simulation by Rogak and Flagan (1990) the ratio $d_H/2r_G$ was computed as a function of N and it was found that the dependence on the primary particle size and N decreased rapidly for $D > 1.3$. For $D \cong 1.79$ the ratio was given as 0.89 for the continuum regime, the same value used in a later simulation (Rogak *et al.*, 1993).

In summary, the literature values for the prefactor and the ratio $d_H/2r_G$, are seen to vary around a value close to unity, but according to the relevant Knudsen regime. The applicability of equation (18) to the continuum regime has been demonstrated while the precise values of the prefactor and $d_H/2r_G$ remain to be determined. Further investigations, under the present experimental conditions, should allow both values to be determined: r_G from scanning electron microscope (SEM) image analysis and ε from a log–log plot of N vs D. However for the present both ε and the ratio $d_H/2r_G$ are assumed to be unity for the sake of clarity.

BERRY THEORY

The terminal settling velocity of an agglomerate was derived by Berry (1989) as part of an assessment on the effect of fractal particles on a nuclear winter. It was argued that for $r_G \gg \lambda$ friction was caused by air flow around the agglomerate and by assuming that the air was entrained inside it. Thus the friction coefficient could be estimated as $F_D/v \cong 3\pi\eta r_G$ and by substituting for r_G from (14), with a pre-factor of unity, the following expression was obtained

$$v_{TS} = \frac{d_0^2 \rho_0 g N^{1-1/D}}{18\eta}(1 + 2\lambda/(d_0 N^{\beta - 1/D})), \tag{21}$$

where $\beta = 1$ if $D < 2$ and $\beta = 2/D$ if $D > 2$. For large agglomerates the terminal settling velocity may be simplified by eliminating the term involving λ, which becomes negligible. The equation predicts that agglomerates of $N = 1000$ and $D = 1.8$ have a terminal settling velocity of $v_{TS} \cong 100\,\text{m y}^{-1}$ as compared to $v_{TS} \cong 1\,\text{km y}^{-1}$ for $D = 3$.

A caloulation of D is possible as all other parameters of interest are known.

Table 1. Theoretical comparison of D_H and D for different aggregation regimes. DLPC = diffusion limited particle–cluster, DLCC = diffusion limited cluster–cluster and RLCC = reaction limited cluster–cluster aggregation

Author	D_H	D	Aggregation regime
Meakin (1983)		2.51 ± 0.06	DLPC
Garik (1985)		2.49 ± 0.19	DLPC
Jullien *et al.* (1984)		1.78 ± 0.05	DLCC
Meakin (1984)		1.76 ± 0.05	DLCC
Kolb and Jullien (1984)		2.00 ± 0.08	RLCC
Brown and Ball (1985)		1.98 ± 0.02	RLCC
Chen *et al.* (1984)	2.13 ± 0.05		DLPC
Meakin *et al.* (1985)	1.84 ± 0.05		DLCC

MAGILL THEORY

The derivation of an expression relating d_{AE} to d_{VE} enabled Magill (1991) to find D whereby d_{GE} was assumed to scale with N, thus

$$N = (d_{GE}/d_0)^D. \tag{22}$$

The following expressions for d_{AE} and d_{GE} were obtained

$$d_{AE} = d_0(\rho_p/\rho_0)^{1/2}(d_{GE}/d_0)^{(D-1)/2}, \tag{23}$$

$$d_{VE} = d_0(d_{GE}/d_0)^{D/3}. \tag{24}$$

Combining equations, (23) and (24),

$$d_{VE} = d_0((\rho_0/\rho_p)^{1/2}(d_{AE}/d_0))^{2D/3(D-1)}. \tag{25}$$

The quantities d_{VE} and d_{AE} are known hence allowing D and d_{GE} to be determined.

NAUMANN AND BUNZ THEORY

In a recent paper by Naumann and Bunz (1991), theoretical equations were derived relating the mobility and mass equivalent diameters of agglomerates for two separate cases: (1) for a step density cut-off at the outer edge of the particle, and (2) for a corresponding exponential cut-off. For a step cut-off

$$d_{ME}\,(\text{step}) = \frac{1.5(D-1)d_0}{D}(f(d_{VE}/d_0)^3)^{1/D}, \tag{26}$$

and for an exponential cut-off, where Γ represents the gamma function

$$d_{ME}(\exp) = (D-1)d_0\left(\frac{f}{\Gamma(D+1)}(d_{VE}/d_0)^3\right)^{1/D}. \tag{27}$$

The parameter f is described as a filling factor, taking into account the occupied space in an agglomerate, and has been given a value of 1.4 for $D \leqslant 2$. When compact particles, such as latex spheres, are considered then $f = 1$.

If both diameters and d_0 are known then D may be calculated using an iterative process, where the Stirling approximation is used to estimate the Gamma function.

APPARATUS

A number of improvements, to the MMC concept of Allen and Raabe (1985a), have allowed a particle to be held in excess of several hours, without electrodynamic containment. Furthermore the use of a CCD camera enables the particle position to be controlled with greater ease. These and other design details will be described in further detail.

Modified Millikan cell

Figure 1 illustrates the MMC in detail. The d.c. plates consist of flat circular and polished brass plates, 7 cm in diameter and with a separation of 1.118 ± 0.001 cm. Various cylindrical inserts may be placed in the MMC to decrease the experimental volume and hence further minimise convection currents. Particles are admitted into the MMC through a 1 mm diameter hole in the upper plate and then exit through a similar exhaust hole in the lower plate. Application of d.c. voltage introduces a vertical electric field between the plates that has negligible fringing at the edges due to the large plate diameter. However due to the holes in the centre of the d.c. plates, the electric field here is theoretically not uniform. Allen and Raabe (1985a) calculated the voltage in the centre of their cell, giving a plate voltage of 999.676 V for the following parameters: a plate distance of 2 cm, plate voltage of 2000 V and a hole diameter of 4 mm. Hence the parameters used in these experiments would similarly introduce a negligible deviation in the calculation of the electric field.

The MMC suspends particles in an inherently unstable equilibrium as the slightest perturbation causes movement in a horizontal direction in the homogeneous electric field. Although convection may be virtually eliminated by insulation, photophoretic forces were found occasionally to significantly perturb the particle position horizontally (due to the particle illumination layout discussed below). The problem may be overcome by superposing an additional containment electric field on the particle, such as that from a Fletcher disc (Fletcher, 1914) or an electrodynamic cell (Wuerker *et al.*, 1959). The latter confinement technique was considered but due to the a.c. restoring force subjected on the particle it was postulated that particle restructuring could occur. Hence the Fletcher disc was deemed more suitable as the restoring force is proportional to the d.c. balance voltage. By applying the balance voltage solely to a 3.5 mm diameter disc, incorporated into the upper d.c. plate, a particle could be restored to its central position within the MMC. Once restored, reapplication of the voltage to the upper d.c. plate was necessary to restore the uniform electric field within the MMC, such that measurements could be made. In this manner particles could be suspended quite easily in excess of several hours.

Convectional forces within the MMC were eliminated by placing the whole MMC within a white enclosure filled with compacted mica insulation chips. Paraffin oil was considered as an insulant but proved unsuitable due to the practical difficulties of working with a liquid.

The main body of the MMC was constructed from Delrin, a black plastic material, due to the ease of machining and good electrical insulation properties. Three ports built into the side of the MMC allowed: (1) the illumination of the particle with a He–Ne laser; (2) illumination with a u.v. light source; and (3) detection with a telescope assembly.

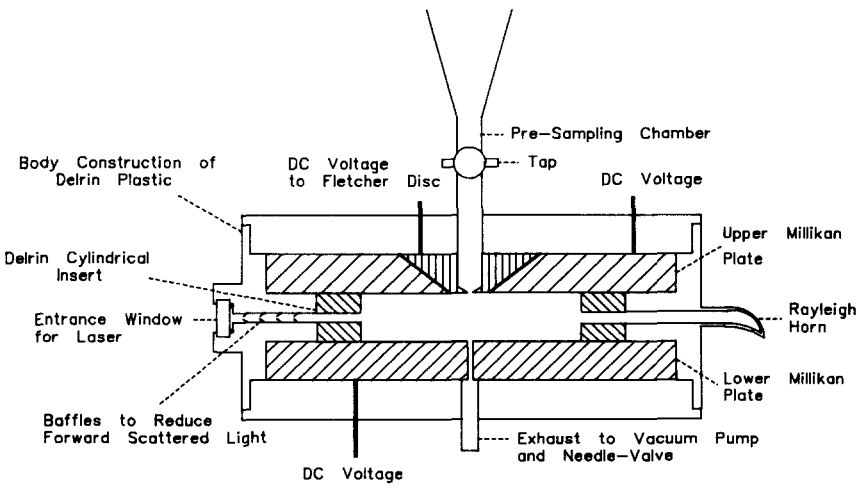

Fig. 1. Detail of the modified Millikan cell.

Situated immediately above the MMC is a conical pre-sampling vessel. The various stop-cocks, on the vessel, isolate an aerosol sample and allow ageing and thermal equilibrium to be attained with the surroundings. Particles may be allowed to sediment by gravity into the MMC which is normally a lengthy procedure. However by careful adjustment of a needle valve attached to the lower plate exhaust hole, a vacuum pump allows particles to be slowly drawn into the MMC. When experimentation has finished the stop-cocks permit the vessel and the MMC to be quickly flushed with filtered air.

Most of the tubing system delivering the particles to the MMC is constructed of glass to avoid loss of charged particles by electrostatic precipitation. Particle charging was unnecessary as particles, of both polarities, were found to be charged to varying degrees.

Particle illumination

Previous investigators (Allen and Raabe, 1985a; Colbeck *et al.*, 1989a) used an illumination configuration whereby the laser beam shone vertically through the Millikan cell. The main disadvantage however was the small illuminated volume resulting in a greater possibility of losing the particle. Instead, an horizontal configuration has been adopted as it allows a beam expander to be easily accommodated into the configuration. By expanding the beam from the 1 mW HeNe laser to approximately 3 mm diameter a suspended particle remains in a large illuminated volume. Should there be any drift, XY adjusters on the beam expander allow the agglomerate to be always optimally illuminated.

Furthermore a horizontal configuration results in only a negligible horizontal photophoresis that may be counteracted by use of the Fletcher disc. In contrast a vertical configuration would introduce a term into equation (1), the force balance equation, that may be difficult to quantify despite Stahlhofen *et al.* (1975) finding no noticeable effect when using either a 2 or 100 mW He–Ne laser.

Particle detection

A schematic of the particle detection system is illustrated in Fig. 2. Light from the particle was detected using a telescope with a focal length of 61 mm mounted on an XYZ adjuster, allowing it to be continuously focused and kept in the centre of the field of view. The angle between the incident and scattered beam was 90°. Although the phase function is a minimum at this angle, particles could be tracked and kept in focus more easily.

Within the telescope the light passes to a CCD camera and a photomultiplier (PM) tube using a 50% beamsplitter. The CCD lens views the particle image through a 15× magnification eyepiece which is then displayed on a high definition monochrome monitor.

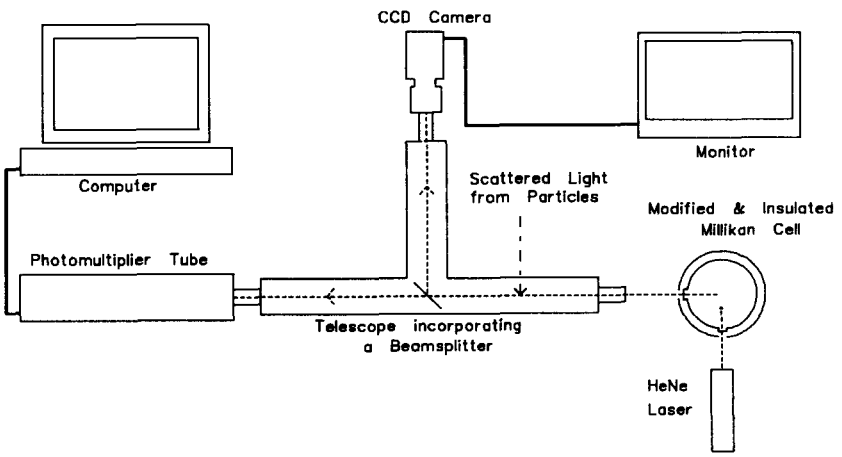

Fig. 2. Schematic of the modified Millikan cell to determine the fractal dimension of carbonaceous agglomerates.

The image received at the Thorn-EMI 9658R PM tube first passes through a 20× magnification eyepiece. Within the eyepiece a transparent rectangular mask, of a determined width, is used to measure the sedimentation time and hence velocity of a particle (Sageev *et al.*, 1986). The PM signal is monitored by an analogue to digital board and acquisition software. Sedimentation times may be determined to an accuracy of greater than 10 ms.

Calibration of the mask width (2.56 mm), was accomplished by measurement against a ruled grating, which gave a true sedimentation distance of 0.413 mm.

Ultra violet light source

A 200 W deuterium lamp and monochromator were used as the u.v. source allowing photon energies up to 7 eV. An iris aperture permitted the intensity to be varied as it was found that photoemission from soot agglomerates occurred readily in contrast to PVT particles which required lengthy exposures at full aperture.

EXPERIMENTAL PROCEDURE

The entire sequence of experimental measurements typically took less than 40 min, which included time to stabilise the MMC and take multiple measurements, although sequences of 15 min are possible. A description of the experimental procedure follows.

(1) For our present studies, it was found that a butane gas burner, with the air inlet blocked off, produced soot agglomerates of a suitable size, up to $d_{AE} \simeq 3$ μm. The butane gas burner was found to have the following properties: 95% elemental carbon content, a sulphate and nitrate content of 0.8 and 0.2% by mass respectively, and a C/H ratio of 59.7 by mass. Hence the primary particle density may be taken as that of amorphous carbon black, 1.8–2.1 g cm^{-3}. In studies by Megaridis and Dobbins (1990), it was found that the primary particles had a uniform size from any position within an ethylene flame with an apparent density of approximately 2 g cm^{-3}. A primary particle density of 2 g cm^{-3} was also reported by Burtscher (1992) and is the value used here.

Soot agglomerates were formed in a chamber, with a volume of 0.195 m^3, which were then subsampled into the glass conical ageing vessel. Typical ageing times chosen were approximately 15 min. During this time the air medium attained thermal equilibrium with the surroundings (important for the reduction of convection in the MMC).

(2) Particles were then drawn into the MMC by careful control of the needle valve. Careful adjustment of the air-flow and the electric field enabled a particle of a certain shape, size and charge to be selected. The precise selection details are described later. Once this had been accomplished the particle was held stationary for at least 10 min to allow: (a) the removal of other particles by collection on the d.c. plates and sedimentation, and (b) for the MMC to achieve a steady state whereby convection did not occur.

(3) The particle was then positioned at the top of the monitor using the electric field and allowed to fall under gravity alone. In order for the particle to adopt its preferred orientation and attain its terminal settling velocity it was allowed to sediment in excess of 5 s before reaching the mask.

The relaxation time (τ) is defined as

$$\tau = v_{TS}/g. \tag{28}$$

A 3 μm PSL sphere has, for example, a time constant of ≅0.03 ms; therefore 5 s was adequate time for the particle to attain its terminal velocity.

Just prior to the particle reaching the mask the software programme was initiated to measure the sedimentation time. At the end of the measurement cycle the particle was then returned to its starting position using the electric field.

(4) After several measurements of v_{TS} under gravity alone, $v_{TS,\|}$ was measured in increasing electric field strengths.

(5) Finally the particle was subjected to u.v. light with the resultant emission of one or more electrons. After each brief exposure to u.v. the new balance voltage, $E_{B,i}$ was measured.

RESULTS AND DISCUSSION

Measurements on 10 soot and 4 PVT particles appear in Tables 2 and 3, respectively. The soot agglomerates were arbitrarily chosen but in order to optimise the experimental procedure the following criteria were applied: (1) an aerodynamic diameter of at least 0.8 μm was chosen, since smaller values encountered difficulties with the measurement of v_{TS} due to Brownian diffusion, and (2) a sufficient charge on the agglomerate was necessary such that low balance voltages were initially required (<200 V) in order to facilitate the u.v. emission technique.

Calculations have been performed with the viscosity and the gas mean free path corrected for temperature and pressure using corrections given by Allen and Raabe (1982). The particle mass was calculated using a linear least-squares fit to the photoemission data and gave regression coefficients greater than 98% in all cases. From this calculation the initial charge on the particle was found. The next column gives the approximate maximum length (L) and perpendicular width (W) of the particle (in μm), measured from the monitor image and calibrated with 2.06 μm PVT particles (standard deviation 0.27 μm). As the image magnification was not sufficient to obtain accurate dimensions a close comparison of these dimensions to χ or D would therefore be inappropriate. However a plot of $(LW)^{0.5}$ vs D suggests a correlation (Samson *et al.*, 1987) which requires more data points than presented here to verify.

Using a primary spherule density of 2 g cm^{-3}, d_{VE} is derived. If the density is taken as unity then the aerodynamic diameter of the volume equivalent sphere, $d_{AE,VE}$, may be compared to the aerodynamic diameter from sedimentation results, d_{AE}. For agglomerates the comparison is not expected to be close whereas for the PVT particles, assuming perfect sphericity, the values are expected to be similar. The close comparison of both d_{AE} and $d_{AE,VE}$ for PVT particles, within experimental error, indicates the negligible convection currents present in the MMC and applicability of the method.

The dynamic shape factor reported for the agglomerates may be compared to previously reported values of χ for soot combustion aerosols (Table 4). Values reported here are seen to

Table 2. Experimental results and derived parameters of carbonaceous agglomerates

Mass (pg)	Initial n	L × W (μm)	d_{VE} (μm)	$d_{AE,VE}$ (μm)	d_{AE} (μm)	$d_{AE,\parallel}$ (μm)	χ	$\chi_{\parallel}$	D
3.32	23	6 × 5	1.47	1.85	1.00	1.29	4.17	2.56	2.14 ± 0.03
3.48	15	8 × 5	1.49	1.86	0.80	0.88	6.41	5.29	1.97 ± 0.03
3.54	40	10 × 4	1.50	1.89	0.90	1.02	5.16	4.11	2.05 ± 0.03
1.12	12	6 × 4	1.03	1.29	0.51	0.63	6.97	4.75	1.87 ± 0.03
3.94	30	5 × 3	1.56	1.96	0.77	1.15	7.41	3.53	1.92 ± 0.03
3.24	27	7 × 5	1.46	1.83	0.94	1.17	4.48	3.01	2.11 ± 0.03
2.19	39	9 × 6	1.28	1.61	0.93	1.25	3.57	2.06	2.19 ± 0.03
11.30	39	9 × 6	2.21	2.78	0.95	1.49	9.93	4.24	1.89 ± 0.03
12.53	50	5 × 4	2.29	2.86	1.19	1.38	6.95	5.19	2.01 ± 0.03
4.14	10	4 × 4	1.58	1.99	0.91	0.94	5.59	5.25	2.03 ± 0.03

Table 3. Experimental results and derived parameters for PVT spheres

Mass (pg)	Initial n	Diam (μm)	d_{VE} (μm)	$d_{AE,VE}$ (μm)	d_{AE} (μm)	$d_{AE,\parallel}$ (μm)	χ	$\chi_{\parallel}$	D
4.67	14	2	2.05	2.07	2.06	2.10	1.02	0.98	2.99 ± 0.03
4.63	28	2	2.05	2.06	2.07	2.12	1.01	0.96	2.99 ± 0.03
4.71	23	2	2.06	2.07	2.03	2.07	1.05	1.01	2.96 ± 0.03
4.95	39	2	2.09	2.11	2.07	2.09	1.05	1.03	2.96 ± 0.03

vary over a larger range than previously reported and may illustrate the effect of re-structuring due to ageing and/or external forces.

In the final column of Tables 2 and 3 the fractal dimension has been calculated with a prefactor $\varepsilon=1$ and a primary spherule diameter of 50 ± 5 nm, measured from SEM images. Most values lie within the range $1.7\leqslant D\leqslant 1.9$ for DLCC growth but as they occur in the upper part of the range linear trajectories are implied (Meakin, 1984b). Such linear impacts may also occur due to differential coagulation, in which agglomerates collide with each other under gravitational sedimentation. Previous investigators have found $D\cong 1.9$ (Colbeck *et al.*, 1989a) and $1.35\leqslant D\leqslant 1.89$ (Katrinak *et al.*, 1993). In a study of the dynamics of solid fractal particles Naumann and Bunz (1992) illustrated the increasing importance of gravitational coagulation as D was decreased. The resulting large enhancement in initial agglomerate growth was unexpected.

A number of agglomerates appeared with $D>2$ for which it was conjectured that restructuring effects were responsible. To illustrate the case two soot particles ($D=2.11$ and 2.19) were deliberately re-structured by reversing the electric field polarity several times and observing the changing morphology on the monitor. In this manner an open structure could be transformed into essentially a spherical structure with ease. It is therefore possible that this mechanism was responsible for the other high observed values of D.

As a verification of the technique and equations utilised PVT particles were used as calibration standards. Table 3 illustrates the results obtained for particles with a number mode of 2.06 μm (verified by SEM analysis). Fractal dimensions vary from 2.96 to 2.99 and show excellent agreement to the theoretical value of 3, hence verifying the method.

An analysis of the error in the calculation of D suggests a value of $D\pm0.03$. When the uncertainty in the soot spherule density and the monomer size are considered then the error, (neglecting the above instrumental error), in the fractal dimension becomes $D\pm0.2$ for $\rho_0=2.0\pm0.1$ g cm^{-3} and $D\pm0.01$ for $d_0=50\pm5$ nm.

Furthermore the effect of varying the prefactor ε and the ratio $d_H/2r_G$ were analysed. For both ε and $d_H/2r_G$ with values of unity D was in the range $1.87\leqslant D\leqslant 2.19$. For $1.1\geqslant\varepsilon\geqslant 0.9$ then D became $1.85\leqslant D\leqslant 2.21$ and for $0.9\leqslant d_H/2r_G\leqslant 1.1$ the result was $1.83\leqslant D\leqslant 2.24$. Although the sensitivity of varying ε and $d_H/2r_G$ within the stated ranges is small, their exact determination nevertheless remains to be made.

A comparison of the present theory and those of other authors is presented in Tables 5 and 6. Close agreement of D, to within an average error of ±0.04, is found for all theories. In the Naumann and Bunz theory the density in the outer region of the particle is described by a step or an exponential cut-off function. The exponential cut-off would appear to give the better description (Naumann, 1993) according to literature results; but as the difference between cut-offs is within experimental error no preference for either can be inferred.

Both cut-offs have been used with a filling factor of 1.4. An analysis of the variation of f in the range $1.35\leqslant f\leqslant 1.45$ gave a variation in D of ±0.009, illustrating the weak dependence on the filling factor.

The close agreement of the above theories can be attributed to the use of equation (14), with alternative characteristic radii and $\varepsilon=1$, in their derivation. For instance equation (26) is similar to equation (15) whereby $\varepsilon=D/(1.5f(D-1))$ and varies in the range $1.07\leqslant\varepsilon\leqslant 0.87$ for $1.8\leqslant D\leqslant 2.2$. In conclusion the overall close comparison of D suggests that the use of different characteristic radii give similar values of D (Tence *et al.*, 1986). Table 7 presents values of the enclosing geometric diameter used in the Berry and Magill

Table 4. Dynamic shape factors of fractal carbonaceous agglomerates

Author	Aerosol soot	Dynamic shape factor χ
Colbeck *et al.* (1989a)	Butane	1.44–3.10
Colbeck *et al.* (1989b)	Butane	4.1–6.3
Colbeck (1990)	Butane	2.2–5.8
This study	Butane	3.6–9.9

Table 5. Comparison of D for carbonaceous agglomerates using the various discussed theories

This study	Magill theory	Berry theory	Naumann and Bunz theory	
			Step ($f=1.4$)	Exp ($f=1.4$)
2.14	2.09	2.15	2.11	2.09
1.97	1.91	1.98	1.91	1.86
2.06	1.99	2.05	2.01	1.98
1.87	1.78	1.86	1.79	1.73
1.93	1.86	1.92	1.86	1.82
2.11	2.05	2.11	2.07	2.05
2.19	2.13	2.19	2.16	2.15
1.89	1.84	1.89	1.83	1.79
2.01	1.97	2.01	1.96	1.94
2.03	1.97	2.03	1.98	1.95

Table 6. Comparison of D for PVT particles using the various discussed theories

This study	Magill theory	Berry theory	Naumann and Bunz theory
			Step ($f=1$)
2.99	2.99	3.00	2.99
2.99	2.99	3.01	2.99
2.96	2.96	2.98	2.96
2.96	2.96	2.98	2.96

theories. While there is some variation of d_{GE} between theories d_{ME} is seen to be lower in all cases as expected.

In Table 8 a comparison is made of D calculated from several different methods for carbonaceous soot. Although the results presented here are somewhat higher they do represent larger agglomerates that have been restructured due to weak van der Waals' forces.

CONCLUSION

A technique has been presented, using established methods, allowing the fractal dimension of a single soot agglomerate to be calculated. The values of D are in close agreement to alternative theories similarly based on the aerodynamic friction experienced by an agglomerate.

The further application of this method and comparison to well established image analysis techniques would require a better knowledge of ε and the exact relation between $2r_G$ and d_H. If the particle in question could be captured on a substrate for SEM analysis then D could be derived in two and three dimensions.

During the experiments electrical restructuring was observed and deliberately carried out on two agglomerates. Various models have been reported which simulate restructuring and readjusting effects present in real aggregation experiments. A simple model investigated by Meakin and Jullien (1988) allowed restructuring immediately after two agglomerates came into contact. For DLCC aggregation D increased from ~ 1.8 to ~ 2.1 and reached ~ 2.2 after the last stage of restructuring. It was found that as restructuring occurred it became increasingly difficult for D to increase. Thus in a similar manner RLCC aggregation only reached $D \sim 2.25$ as the initial value was relatively higher at $D \sim 2.0$. Although electrical restructuring mechanisms were not considered, it is seen that simple restructuring mechanisms lead to increases in D.

Table 7. Calculated values of the mobility equivalent diameter in comparison to the enclosing geometric sphere diameter for the Berry and Magill theories

Present study d_{ME} (μm)	Berry theory d_{GE} (μm)	Magill theory d_{GE} (μm)
5.66	7.63	6.73
8.77	12.51	10.54
7.14	9.95	8.61
6.33	9.84	7.65
10.58	15.25	12.68
6.03	8.32	7.27
4.2	5.74	5.05
20.54	28.80	24.64
14.97	20.29	17.98
8.17	11.39	9.86

Table 8. Reported values of the fractal dimension for carbonaceous agglomerates (TEM = transmission electron microscope, LS = light scattering and MMC = modified Millikan cell)

Author	Aerosol soot	Agglomerate size (μm)	Primary	Method	Fractal dimension
Samson *et al.* (1987)	Acetylene	<1.0	30	TEM	1.5–1.6
Zhang *et al.* (1988)	Methane	1–5	20	LS	1.62 ± 0.06
				TEM	1.72 ± 0.10
Colbeck *et al.* (1989a)	Butane	$\leqslant 20$	60	MMC	1.9
Megaridis and Dobbins (1990)	Ethene	<0.9	10–40	LS	1.62 ± 0.04
Gangopadhyay *et al.* (1991)	Methane	<0.12	30	LS	1.6–1.8
This study	Butane	$\leqslant 10$	50	MMC	1.87–2.19

Important areas for the implications of agglomerate re-structuring, identified by Jullien and Meakin (1989) were rheology, the nuclear winter scenario (Berry and Percival, 1986) and air and water pollution. Using the method presented here D may be measured for a variety of materials and the effects of restructuring on agglomerates may also be observed. The ability to measure and monitor D for single particles allows their microchemical–physical properties to be investigated. The technique may be of particular relevance to investigating the fate of carbonaceous aerosols released to the atmosphere. Such aerosols are poorly characterised and may potentially have a detectable impact on the global climate (US Dept. Energy, 1993). Restructuring phenomena have a direct influence on agglomerate atmospheric lifetimes and optical properties, hence the importance of determining their microchemical–physical properties are recognised.

Acknowledgements—The authors are grateful to the Leverhulme Trust and SERC for financial support of this work.

REFERENCES

Allen, M. D. and Raabe, O. G. (1982) Re-evaluation of Millikan's oil drop data for the motion of small particles in air. *J. Aerosol Sci.* **13,** 537.

Allen, M. D. and Raabe, O. G. (1985a) Slip correction measurements of spherical solid aerosol particles in an improved Millikan apparatus. *Aerosol Sci. Technol.* **4,** 269.

Allen, M. D. and Raabe, O. G. (1985b) Slip correction measurements for aerosol particles of doublet and triangular triplet aggregates of spheres. *J. Aerosol Sci.* **16,** 57.

Arnold, S. (1979) Determination of particle mass and charge by one electron differentials. *J. Aerosol Sci.* **10,** 49.

Berry, M. V. (1989) Falling fractal flakes. *Physica D* **38,** 29.

Berry, M. V. and Percival, I. C. (1986) Optics of fractal clusters such as smoke. *Optica Acta* **33,** 577.

Bolle, G., Cametti, C., Codastefano, P. and Tartaglia, P. (1987) Kinetics of salt-induced aggregation in polystyrene lattices studied by quasielastic light scattering. *Phys. Rev. A.* **35,** 837.

Brown, W. D. and Ball, R. C. (1985) Computer simulations of chemically limited aggregation. *J. Phys. A.* **18,** L517.

Burtscher, H. (1992) Measurement and characteristics of combustion aerosols with special consideration of photoelectric charging and charging by flame ions. *J. Aerosol Sci.* **23,** 549.

Cametti, C., Codastefano, P. and Tartaglia, P. (1987) Light scattering measurements of slow aggregation in colloids: deviation from asymptotic time scaling. *Phys. Rev. A.* **36,** 4916.
Cargill, G. S. (1984) In *Physics and Chemistry of Porous Media* (Edited by Johnson, D. L. and Sen, P. N.). SIP, New York.
Chen, Z. Y., Deutch, J. M. and Meakin, P. (1984) Translational diffusion coefficient of diffusion limited aggregates. *J. Chem. Phys.* **80,** 2982.
Chen, Z. Y., Meakin, P. and Deutch, J. M. (1987) Comment on "Hydrodynamic behavior of fractal aggregates". *Phys. Rev. Lett.* **59,** 2121.
Cheng, Y. S., Allen, M. D., Gallegos, D. P., Yeh, H. C. and Peterson, K. (1988) Drag force and slip correction of aggregate aerosols. *Aerosol Sci. Technol.* **8,** 199.
Colbeck, I. (1990) Dynamic shape factors of fractal clusters of carbonaceous smoke. *J. Aerosol Sci.* **21,** S43.
Colbeck, I., Appleby, L., Hardman, E. J. and Harrison, R. M. (1990) The optical properties and morphology of cloud-processed carbonaceous smoke. *J. Aerosol Sci.* **21,** 527.
Colbeck, I., Eleftheriadis, K. and Simons, S. (1989a) The dynamics and structure of smoke aerosols. *J. Aerosol Sci.* **20,** 875.
Colbeck, I., Hardman, E. J. and Harrison, R. M. (1989b) Optical and dynamical properties of fractal clusters of carbonaceous smoke. *J. Aerosol Sci.* **20,** 765.
Dahneke, B. E. (1973) Slip correction factors for non-spherical bodies III. The form of the general law. *J. Aerosol Sci.* **4,** 163.
Fletcher, H. (1914) A determination of Avogadro's constant N from measurements of the Brownian movements of small oil drops suspended in air. *Phys. Rev.* **4,** 440.
Forrest, S. R. and Witten, T. A. (1979) Long-range correlations in smoke-particle aggregates. *J. Phys. A.* **12,** L109.
Gangopadhyay, S., Elminyawi, I. and Sorensen, C. M. (1991) Optical structure factor measurements of soot particles in a premixed flame. *Appl. Optics* **30,** 4859.
Garik, P. (1985) Anisotropic growth of diffusion-limited aggregates. *Phys. Rev. A.* **32,** 1275.
Gentry, J. W., Mulholland, G. W. and Sullivan, F. (1988) In *Atmospheric Aerosols and Nucleation* (Edited by Wagner, P. and Vali, G.), pp. 116–119. Springer-Verlag, Berlin.
Hess, W., Frish, H. L. and Klein, R. (1986) On the hydrodynamic behaviour of colloidal aggregates. *Z. Phys. B-Condensed Matter* **64,** 65.
Hinds, W. C. (1982) *Aerosol Technology.* Wiley, New York.
Hurd, A. J. and Flower, W. L. (1988) *In situ* growth and structure of fractal silical aggregates in a flame. *J. Colloid Int. Sci.* **122,** 178.
Jagoda, I. J., Prado, G. and Lahaye, J. (1980) An experimental investigation into soot formation and distribution in polymer diffusion flames. *Comb. Flame* **37,** 261.
Jullien, R., Kolb, M. and Botet, R. (1984) Aggregation by kinetic clustering of clusters in dimensions $d > 2$. *J. Phys.* **45,** L211.
Jullien, R. and Meakin, P. (1989) Simple models for the re-structuring of 3D ballistic aggregates. *J. Colloid Int. Sci.* **127,** 265.
Kasper, G. (1982) Dynamics and measurement of smokes. I. Size characterisation of nonspherical particles. *Aerosol Sci. Technol.* **1,** 187.
Katrinak, K. A., Rez, P., Perkes, P. R. and Buseck, P. R. (1993) Fractal geometry of carbonaceous aggregates from an urban aerosol. *Envir. Sci. Technol.* **27,** 539.
Kaye, B. H. (1984) Multifractal description of a rugged fine particle profile. *Part. Charact.* **1,** 14.
Kaye, B. H., Clark, G. C., Leblanc, J. K. and Trottier, R. A. (1987) Image analysis procedures for characterizing the fractal dimension of fine particles. *Part. Charact.* **4,** 63.
Kolb, M. and Jullien, R. (1984) Chemically limited versus diffusion-limited aggregation. *J. Phys. Lett.* **45,** 977.
Kütz, S. and Schmidt-Ott, A. (1990) Use of a low-pressure impactor for fractal analysis of submicron particles. *J. Aerosol Sci.* **21,** S47.
Magill, J. (1991) Fractal dimension and aerosol particle dynamics. *J. Aerosol Sci.* **22,** S165.
Martin, J. E., Schaefer, D. W. and Hurd, A. J. (1986) Fractal geometry of vapor-phase aggregates. *Phys. Rev. A.* **33,** 3540.
Meakin, P. (1983) Diffusion-controlled cluster formation in 2–6 dimensional space. *Phys. Rev. A.* **27,** 1495.
Meakin, P. (1984a) Diffusion limited aggregates in three dimensions: results from a new cluster–cluster aggregate model. *J. Colloid Int. Sci.* **102,** 491.
Meakin, P. (1984b) Effects of cluster trajectories on cluster–cluster aggregation: A comparison of linear and Brownian trajectories in two- and three-dimensional simulations. *Phys. Rev. A.* **29,** 997.
Meakin, P., Chen, Z. Y. and Deutch, J. M. (1985) The translational diffusion coefficient and time dependent cluster size distribution of three-dimensional cluster–cluster aggregation. *J. Chem. Phys.* **82,** 3786.
Meakin, P. and Jullien, R. (1988) The effects of restructuring in the geometry of clusters formed by diffusion limited, ballistic, and reaction-limited cluster–cluster aggregation. *J. Chem. Phys.* **89,** 246.
Megaridis, C. M. and Dobbins, R. A. (1990) Morphological description of flame-generated materials. *Combust. Sci. Technol.* **71,** 95.
Mountain, R. D. and Mulholland, G. W. (1984) in *Kinetics of Aggregation and Gelation: Proceedings of the International Topical Conference* (Edited by Family, F. and Landau, D. P.). North Holland, Amsterdam.
Mountain, R. D. and Mulholland, G. W. (1988) Light scattering from simulated agglomerates. Langmuir **4,** 1321.
Mountain, R. D., Mulholland, G. W. and Baum, H. (1986) Simulation of aerosol agglomeration in the free molecular and continuum flow regimes. *J. Colloid Int. Sci.* **114,** 67.
Mulholland, G. W., Samson, R. J., Mountain, R. D. and Ernst, M. H. (1988) Cluster size distribution for free molecular aggregation. *J. Energy Fuels* **2,** 481.
Naumann, K. H. (1993) Personal communication.
Naumann, K. H. and Bunz, H. (1991) Aerodynamic properties of fractal aerosol particles. *J. Aerosol Sci.* **22,** S161.
Naumann, K. H. and Bunz, H. (1992) Computer simulations on the dynamics of fractal aerosols. *J. Aerosol Sci.* **23,** S361.

Philip, M. A., Gelbard, F. and Arnold, S. (1983) An absolute method for aerosol particle mass and charge measurement. *J. Colloid Int. Sci.* **91,** 507.

Rarity, J. G. and Pusey, P. N. (1986) Light scattering from aggregating systems: static, dynamic (QELS) and number fluctuations. In *On Growth and Form* (Edited by Stanley, H. E. and Ostrowsky, N.). Martinus Nijhoff, Dordrecht.

Rogak, S. N. and Flagan, R. C. (1990) Stokes drag on self-similar clusters of spheres. *J. Colloid Int. Sci.* **134,** 206.

Rogak, S. N., Flagan, R. C. and Nguyen, H. V. (1993) The mobility and structure of aerosol agglomerates. *Aerosol Sci. Technol.* **18,** 25.

Sageev, G., Seinfeld, J. H. and Flagan, R. C. (1986) Particle sizing in the electrodynamic balance. *Rev. Sci. Instrum.* **57,** 933.

Samson, R. J., Mulholland, G. W. and Gentry, J. W. (1987) Structural analysis of soot agglomerates. *Langmuir* **3,** 272.

Schaefer, D. W., Martin, J. E., Wiltzius, P. and Cannell, D. S. (1984) Fractal geometry of colloidal aggregates. *Phys. Rev. Lett.* **52,** 2371.

Schmidt-Ott, A. (1988a) *In situ* measurement of the fractal dimensionality of ultrafine aerosol particles. *Appl. Phys. Lett.* **52,** 954.

Schmidt-Ott, A. (1988b) New approaches to *in situ* characterization of ultrafine agglomerates. *J. Aerosol Sci.* **19,** 553.

Sorensen, C. M., Cai, J. and Lu, N. (1992) Light scattering measurements of monomer size, monomers per aggregate, and fractal dimension for soot aggregates in flames. *Appl. Optics* **31,** 6547.

Stahlhofen, W., Armbruster, Gebhart, J. and Grein, E. (1975) Particle sizing of aerosols by single particle observation in a sedimentation cell. *Atmos. Envir.* **9,** 851.

Tence, M., Chevalier, J. P. and Jullien, R. (1986) On the measurement of the fractal dimension of aggregated particles by electron microscopy: experimental method, corrections and comparison with numerical models. *J. Phys.* **47,** 1989.

US Dept. Energy, (1993) Quantifying and minimizing uncertainty of climate forcing by anthropogenic aerosols. DOE/NBB-0092T, Env. Sci. Div., Washington D.C. 20585, U.S.A.

van Saarlos, W. (1987) On the hydrodynamic radius of fractal aggregates. *Physica A.* **147,** 280.

Weber, A. P. (1992) Characterization of the geometrical properties of agglomerated aerosol particles. Paul Scherrer Institute report Nos. 129, Villigen, Switzerland.

Wiltzius, P. (1987) Hydrodynamic behaviour of fractal aggregates. *Phys. Rev. Lett.* **58,** 710.

Wuerker, R. F., Shelton H. and Lagmuir, R. V. (1959) Electrodynamic containment of charged particles. *J. appl. Phys.* **30,** 342.

Zhang, H. X., Sorensen, C. M., Ramer, E. R., Oliver, R. J. and Merklin, J. F. (1988) *In situ* optical structure factor measurements of an aggregating soot aerosol. *Langmuir* **4,** 867.